2023

The Effect of Mild Traumatic Brain Injury on Perineuronal Nets Surrounding Neocortical Parvalbumin Interneurons

Olivia Lowman
Virginia Commonwealth University

The Effect of Mild Traumatic Brain Injury on Perineuronal Nets Surrounding Neocortical Parvalbumin Interneurons

A thesis/dissertation submitted in partial fulfillment of the requirements for the degree of Masters of Anatomy and Neurobiology at Virginia Commonwealth University.

By:

Olivia A. Lowman
Bachelor of Science, The University of Tennessee, 2019

Advisor: Kimberle M. Jacobs
Associate Professor
Virginia Commonwealth University
Richmond, Virginia
August 2023

Acknowledgments

I would like to thank my friends and family for all the support they have given me during my time in school. My mentors Dr. Kimberle Jacobs and Dr. John Greer for providing me with the most insight, guidance, and expertise. Also, Dr. Jeffrey Dupree for your support of this project. All of the lab members, especially Alan Harris for helping me switch from being an engineer to a neuroscience student. The knowledge and experience I have gained working in this lab will forever help me in furthering my studies and education. And finally, Virginia Commonwealth University for giving me the option to pursue this degree.

TABLE OF CONTENTS

ABSTRACT 4
INTRODUCTION 5
MATERIALS AND METHODS 13
RESULTS 17
DISCUSSION 29
BIBLIOGRAPHY 34

TABLE OF FIGURES

Figure 1 18
Figure 2 19
Figure 3 21
Figure 4 21
Figure 5 22
Figure 6 24
Figure 7 26
Figure 8 28
Figure 9 28

ABSTRACT

Mild traumatic brain injury (mTBI) is an extremely common affliction with an estimated 42 million people being affected by it worldwide each year. It can lead to a range of long-term chronic issues and the underlying pathology is not well understood. Several previous studies have shown that parvalbumin inhibitory interneurons (PV+) are injured during TBI, therefore altering the excitatory to inhibitory ratio in neural networks which can lead to several neurodegenerative disorders such as epilepsy. Perineuronal nets (PNNs) are an extracellular matrix element that preferentially surround PV+ neurons in the neocortex and are recently thought to have important roles in neuroplasticity and may serve as protection for PV+ neurons. While several studies have previously examined how PNNs are affected after injury, all of these studies have either focused on the hippocampus or have a severe injury level indicating contusion. The central fluid percussion injury model used for this study was created to model mTBI without contusion, as a diagnosis in humans lacks contusion injury. In this study, we were able to confirm a reduction of PNNs around some PV+ cells in the neocortex after mTBI without contusion injury. We were also able to show that the majority of axotomized PV+ cells were either surrounded by little WFA or no WFA staining indicating the majority of injured PV+ cells have weak or no PNNs present.

INTRODUCTION

Mild traumatic brain injury (mTBI) can be classified as acute brain dysfunction due to impact forces or rapid acceleration/deceleration which lead to a variety of cognitive and physical symptoms (Katz, Cohen, & Alexander, 2015)While it can be difficult to know the actual number of mTBI cases per year due to a wide range of present symptoms as well as a spectrum of severity of symptoms, leading to some patients not seeking medical attention, it can be estimated that roughly 600 per 100,000, or around 42 million people globally, are affected by mTBI each year (Gardner & Yaffe, 2015) The large range of cognitive and physical symptoms can also make diagnoses difficult. One of the most widely accepted diagnostic criterion models comes from the American Congress of Rehabilitation Medicine (Silverberg et al., 2023). Clinical criteria can include loss of consciousness immediately following injury, complete or partial amnesia immediately after injury, or alteration of mental status immediately after injury. Physical symptoms can include problems with vision and balance, dizziness, sensitivity to light and noise, and/or nausea and vomiting. Common cognitive symptoms include mental fog, difficulty concentrating, problems with memory, or uncharacteristic emotional state such as excess irritability. Neuroimaging can be used as a diagnostic tool but is not required for official diagnosis, as it is mostly used to assess injury greater than mTBI. “Mild” TBI is not given as a diagnosis if unconsciousness lasts longer than 30 minutes after injury or amnesia lasts for more than 24 hours after injury, these longer lasting symptoms indicate the need to upgrade the diagnosis to severe TBI. Repeated exposure to mTBI can increase the severity of symptoms over time which also results in longer recovery time, this is most commonly seen in those that have experienced multiple concussion injuries. This repeated exposure can also lead to long term symptoms persisting more than three months after the initial injury such as long-term issues with

memory and/or attention, constant headaches, and trouble with regulation of emotion. In these cases, diagnosis is often increased from mTBI to post-concussion syndrome (Kelly, Amerson, & Barth, 2012). Treatment of mTBI is often quite simple, over the counter anti-inflammatories to ease pain and rest from normal activity until symptoms subside. It is recommended to receive care from a healthcare provider if symptoms persist past three months of the injury (Prince & Bruhns, 2017).

In order to replicate mTBI, the central fluid percussion injury model (cFPI) was used for this study. cFPI is one of the oldest and most well studied injury models that consists of an extremely reproducible surgery that is able to model a concussive injury (Kabadi, Hilton, Stoica, Zapple, & Faden, 2010). One of the most important aspects of this injury model is that it does not create a serious brain contusion that often results in cell death (Rowe, Harrison, Ellis, Adelson, & Lifshitz, 2018). Survival of the animal and the return of normal motor function after injury are also important conditions of this model in order to represent concussion injuries in humans. While cFPI does not include a large contusion injury, it does result in axonal injury.

Traumatic axonal injury (TAI) is a common component of mTBI with the injury being visually represented by evident swellings, called bulbs, located near the axonal initial segment (AIS) when viewed microscopically (J.E. Greer, Hanell, & Jacobs, 2013). While brain tissue is quite elastic and normal movement results in some stretching of the axon, inertial forces from brain injury results in rapid tensile elongation of axons which can damage the cytoskeleton resulting in injury (Smith, Meaney, & Shull, 2003) The swollen bulbs that come with axonal injury hail from a swift influx of sodium and calcium into the axon due to permeability changes (Li, Mealing, Morley, & Stys, 1999; Lusardi, Wolf, Putt, Smith, & Meaney, 2004). Within the bulbs, there is an accumulation of axonal transport proteins caused by damage to the

cytoskeleton of the axon. As these bulbs can only be viewed microscopically, it is extremely difficult to know if a patient has axonal injury after mTBI; very few treatment procedures for mTBI have been geared towards injury to the axon. Calpain inhibitors have been shown to reduce the loss of neurofilament proteins that makeup the axonal cytoskeleton which can protect the axon from breaking down. However, these inhibitors are difficult to administer so their use is not very practical (Posmantur et al., 1997). Further research must be done to find treatment for axonal injury after mTBI. Until recently, it was thought that only white matter, containing mainly excitatory neurons, was susceptible to TAI. It has been recently discovered that GABAergic inhibitory neurons are also susceptible to TAI after mTBI. In fact, it has been found that around 10% of GABAergic neurons in the neocortex were axotomized after injury (Vascak, Jin, Jacobs, & Povlishock, 2018), similar to the number of axotomized YFP-h excitatory layer V pyramidal neurons previously identified using the same cFPI model (J.E. Greer, Povlishock, & Jacobs, 2011). Within the population of axotomized GABAergic neurons 82% were Parvalbumin (PV+) interneurons (Vascak et al., 2018). This recent finding suggests that the PV subpopulation may be particularly vulnerable while other inhibitory subtypes are resilient. Thus, one goal of the Greer and Jacobs labs is to identify the underlying neuronal mechanisms for this vulnerability.

Several types of inhibitory interneurons are found in the cortex region of the brain, each one has its own unique characteristics and roles in cortical networks, they can be differentiated by aspects such as firing patterns and morphology. PV+ is a calcium binding protein that can be found in various regions of the brain including the hippocampus, cerebellum, and reticular thalamus. In the cortex, PV+ expressing cells are fast spiking GABAergic inhibitory interneurons that control the output of pyramidal cells into cortical networks. They are usually composed of chandelier and basket cell morphological types (Miyamae, Chen, Lewis, & Gonzalez-Burgos,

2017). It has been suggested that PV+ is a modulator of calcium movement between synapses which can have an impact on both amplitude and time course of calcium in synapse terminals following an action potential. In a study involving PV knockout mice (PV-), wild type (PV+/PV+) mice showed paired pulse depression while the knockout mice (PV-/PV-) showed paired pulse facilitation as a response of residual calcium. This shows the stark impact PV+ has on the short term plasticity of GABAergic neurons (Caillard et al., 2000). Fast spiking GABAergic neurons are positive for PV+ and negative for somatostatin, another common subtype of interneuron found in the cortex. (Karube, Kubota, & Kawaguchi, 2004). Not only are there large morphological differences between PV+ and somatostatin GABAergic neurons, but there are also distinct differences in function. A large role of both types of these inhibitory interneurons is to synchronize action potential spike times across the layers of the cortex. While PV+ neurons preferentially synchronize spike rates when the network activity is firing at low frequencies, somatostatin does the opposite and synchronizes when the network activity has high spike frequencies (Jang et al., 2020). Furthermore, PV+ neurons contribute to feedforward inhibition while somatostatin neurons contribute to feedback inhibition (Jang et al., 2020). Feedforward inhibition occurs when an excitatory neuron activates both excitatory and inhibitory neurons in their circuit allowing the inhibitory neurons to control the level of output. Feedback inhibition works by a principal excitatory neuron activating an inhibitory neuron which in turn inhibits the principal cell (Kee, Sanda, Gupta, Stopfer, & Bazhenov, 2015). Having different cell types to control different ranges of firing frequencies as well as both types of inhibition allows for fine control of the synchronization of spiking, disruptions of this synchronization due to significant loss of interneurons is well known to be associated with seizure disorders (Cardin, 2018; Menuz & Nicoll, 2008; Sayin, Osting, Hagen, Rutecki, & Sutula, 2003). Seizure disorder

due to loss of inhibition arises from the change in balance of excitatory to inhibitory signaling. Loss of interneurons can come from a variety of neurological problems such as traumatic injury, genetic disorder, and environmental toxins (Hutchins & Barger, 1998).

For this study, the distinction between classes of GABAergic interneurons becomes especially important when examining the presence of PNNs. While somatostatin cells are also a prevalent type of GABAergic cell in the cortex, they completely lack PNNs. In fact, one study that produced cells that express PV+ and somatostatin showed that any cell containing somatostatin always lacks PNNs even if they are positive for PV+ (Miao, Cao, Moser, & Moser, 2017). This further reinforces that PNNs specifically surround fast spiking PV+ neurons in the cortex. PNNs were first discovered by Camillo Golgi in the late 1800s when he described them as a "delicate covering" in his now famous images of the nervous system. They were basically ignored for a long period of time until their presence was officially recognized in the 1970s (Shen, 2018). Today, we know PNNs to be chondroitin sulfate proteoglycan containing extracellular matrix structures that are found in many areas of the brain around a variety of different cell types. In the cortex, they preferentially surround the soma and dendrites of PV+ neurons (Fawcett, Oohashi, & Pizzorusso, 2019; Sorg et al., 2016; Yang et al., 2021). While the exact role of PNNs was widely unknown for years after their discovery, it has been recently established that they have a large role in neuroplasticity, as they develop as a sign of the end of the critical period during development. PNNs have been described as a "net-like" structure due to the holes that have been observed in the framework. Synaptic boutons have been shown to reside in these holes within the nets and this is thought to be how the PNNs are able to control plasticity (Sigal, Bae, Bogart, Hensch, & Zhuang, 2019). This study done by Sigal, used Syt2, which is an axon terminal marker specific to PV+ cells, to visualize how mature PNNs are able

to restrict synaptic plasticity. Syt2+ boutons were observed to have some overlap with the surface of PNNs on the area surrounding the holes in the nets. When younger mice (P30) were compared to older mice (P90), the older mice, having more mature PNNs, were shown to have a significantly larger area of Syt2+ surface overlap suggesting that the PNNs are able to "pin" the synaptic boutons in place. This would not only restrict the movement of synapses around the cell, but also prevent new synapses from forming due to the increased rigidity of the mature PNNs. Now, researchers are using drug induced loss of PNNs to reintroduce neuroplasticity in a wide range of applications such as aiding in memory retention, (Dubisova et al., 2022) and reducing drug seeking behavior during addiction (Brown & Sorg, 2023). While losing PNNs can result in the reintroduction of plasticity, it has also been linked to several neurodegenerative disorders such as Alzheimer's Disease and epilepsy (Baig, Wilcock, & Love, 2005; Crapser et al., 2020; Rankin-Gee et al., 2015). The mechanisms as to how PNNs control neuroplasticity are clearly still not understood as it seems contradictory that in some cases the loss can aid in memory retention and in others reduce memory retention. It is thought that there must be some sort of delicate balance between when the amount of PNNs lost has a positive effect versus a negative effect, but at what point exactly the scales tip from helpful to harmful is still unknown (Bosiacki et al., 2019).

A newly proposed role of PNNs is an ion transport barrier which would have a direct impact on the diffusion of charged particles across membranes (Hanssen & Malthe-Sorenssen, 2022). The anionic charge density of PNNs due to the glycosaminoglycan chains may allow them to compartmentalize important ions such as K+ and Ca2+ meaning that they would be able to influence synaptic gradients. Surface compartmentalization would allow neurons to adjust synaptic responses on just their surface thus not affecting any neighboring cells, (Frischknecht et

al., 2009) this could be another way that PV+/PNN+ cells would have fine control over inhibition in cell networks. One study was able to show that injecting the enzyme chondroitinase cleaves the negatively charged particles of PNNs which lead to the facilitation of diffusion (Hrabetova, Masri, Tao, Xiao, & Nicholson, 2009). On the other hand, the addition of hyaluronic acid, the main glycosaminoglycan component of PNNs, did the opposite and hindered diffusion (Morawski et al., 2015). While these studies had opposite results due to their methodology, they can come to the same conclusion that PNNs have an effect on diffusion rates due to their anionic properties.

Another suggested role of PNNs is neuroprotection from toxic environments. As fast spiking neurons, PV+ cells have a higher metabolic need shown by their increased density of mitochondria, (Lichvarova, Henzi, Safiulina, Kaasik, & Schwaller, 2018) this leaves them particularly vulnerable to oxidative stress not seen in other types of inhibitory interneurons. Oxidative stress can also come from environmental toxins such as exposure to air pollutants which is an increasing issue to those that live in urban areas (Hong et al., 2009). Neurodegenerative disorders, especially schizophrenia, have also been proven to increase oxidative stress in the brain due to an altered antioxidant response from lower levels of antioxidant regulator glutathione (Do et al., 2000). Chondroitin sulfate, one of the main components of PNNs has been shown to reduce reactive oxygen species (ROS) formed from mitochondrial disruption, this suggests that PNNs can act as a protective barrier around PV+ cells by neutralizing ROS before they are able to reach the neuron (Canas et al., 2007). As previously discussed, PNNs are able to compartmentalize certain cations such as calcium and potassium, another cation they have been seen to compartmentalize is iron. Iron has been shown to catalyze the reaction of hydrogen peroxide to ROS which could leave the cell exposed to

oxidative stress. As a measure to protect themselves from oxidative stress due to one of their own functions, chondroitin sulfate aggregates around the net can collect iron ions and reduce the accumulation intracellularly (Morawski, Bruckner, Riederer, Bruckner, & Arendt, 2004). To show that PNNs are able to shield fast spiking PV+ cells from oxidative stress, one study examined damage from ROS due to increased oxidative stress in young mice (P20) compared to more mature mice (P90). Since the presence of PNNs is a hallmark of the end of neuroplasticity in mature animals, the younger mice would have less PNNs in general as well as not fully formed PNNs. A dopamine reuptake inhibitor was injected into the mice increasing levels of dopamine, therefore increasing the amount of ROS present in the brain. Both ages of mice were subject to severe oxidative stress but only the younger mice were found to have a decreased amount of PV+ cells (Cabungcal et al., 2013). All of these roles of PNNs show that they have a large impact on maintaining properly functioning neural networks. Since it has been shown that after mTBI, there can be a loss of functioning neural networks, this study aims to determine if there is an impact on PNNs after injury.

Several histological approaches can be used to visualize PNNs including *vica villosa* agglutinin and soybean agglutinin, currently, the most widely used approach, and the approach used in this study, is the use of *wisteria floribunda* agglutinin (WFA) (Hartig, Meinicke, Michalski, Schob, & Jager, 2022). WFA is a lectin that is able to uniquely bind to the terminal N-acetyl galactosamine residues in PNNs making the entire net easily visible without staining any neighboring structures (Ajmo, Eakin, Hamel, & Gottschall, 2008). It has been well established that there is a positive correlation between WFA staining intensity and PNN maturity with the staining intensity of WFA increasing as the PNN becomes more mature (Carstens, Phillips, Pozzo-Miller, Weinberg, & Dudek, 2016; Hobohm et al., 2005; Slaker, Harkness, &

Sorg, 2016). This feature of using WFA as a PNN marker is extremely useful for quantifying PNN maturity. As previously discussed in detail, more mature PNNs are thought to provide a high level of protection to the cells they surround as well as having a role in maintaining proper levels of inhibition to neural networks. Being able to determine PNN maturity from staining allows for this study to establish if PV+ cells with more or less mature PNNs are susceptible to TAI.

MATERIALS AND METHODS

INJURY MODEL

The central fluid percussion injury has been described in detail in a previous paper from John Greer (J. E. Greer, Hanell, McGinn, & Povlishock, 2013). Briefly, male or female RxPV mice aged 10-12 weeks were anesthetized with 4% isoflurane and a craniotomy is made between the bregma and lambda. A syringe hub was attached to the craniotomy site using cyanoacrylate and stabilized using dental glue. Mice were allowed to recover around 60 minutes and then are re-anesthetized again with 4% isoflurane for the fluid injury. The attached hub was filled with 0.9% saline and connected to the male end of the fluid apparatus. Brief pressure was placed upon the dura to give a moderate injury by a pendulum hitting a fluid filled piston at 1.6 +/- 0.4 atms. The hub is then removed from the animal and they were sutured and allowed to recover. For sham animals, the process is repeated the same way but without the mild injury. Following the injury, mice were given 3 hours to recover (RxPV sham n=2; 3 hours, n=8;) (TdxPV Naive n=1) At 3 hours, mice were placed in a chamber with around 1ml 4% isoflurane until cessation of breathing. They were then transcardially perfused with 0.9% saline solution for 2 minutes

followed by 4% paraformaldehyde in 0.9% saline for 7 minutes. After perfusion, the brain was removed and suspended in the paraformaldehyde solution for 24 hours in 4 degrees C. Brains were switched over to 0.1M PBS buffer after 24 hours until slicing. For slicing, the brains were blocked coronally at the optic chiasm and midbrain so that when mounted, the piece included the parietal and temporal cortices, hippocampus, and thalamus. Brains were mounted using cyanoacrylate and covered in 0.1M PBS. Sections were cut at a thickness of 50 microns using a vibratome (Leica VT1000S; Leica Microsystems, Bannockburn, IL, USA). Collection of sections started at the emergence of the hippocampus and ended before the emergence of the cerebral aqueduct and placed in 0.1M PBS in a 24 well culture plate.

EXPERIMENTAL ANIMALS

All animals were received from Jackson Laboratories. Rho strains [B6.Cg-Gt(ROSA)26Sor, stock number 024109, Bar Harbor, ME, United States] were mated with PV-cre mice (B6.129P2-Pvalb, stock number 017320) in order to make the RxPV mice that were used for the majority of the study. The other mice that were bred were TdxPV mice using the same PV-cre mice and Td-tomato strains [B6.Cg-Gt(ROSA)26Sor, stock number 007909]. All animal procedures were approved by the institutional animal care and use committee of Virginia Commonwealth University.

IMMUNOHISTOCHEMISTRY

Previous work showed that immunohistochemical staining for the GABA synthetic enzyme, glutamic acid decarboxylase (GAD) was useful in identifying axotomized inhibitory interneurons after cFPI. Thus, we utilized the same staining in order to find axotomized neurons in the current project. In addition, we expected to identify PV among the different GABAergic subtypes via the use of the RxPV strain. Finally, we stained for WFA to identify the status of the

PNN on the GABAergic interneurons. Sections for staining and imaging of the RxPV mouse strain were selected by observing the emergence of the hippocampus for the first section and then selecting the next section from 5 well plates ahead so that each section analyzed was 200 microns apart. A total of 5 sections were collected from each animal . Primary antibodies included mouse GAD67 (1:1000; Millipore MAB5406), biotinylated WFA (1:200; Vector Labs B-1355), and chicken GFP (1:1000; Millipore 06-896). General immunostaining protocol was as follows; slices were first washed in a 0.1M PBS buffer 3 times for 10 minutes each wash. A solution of 0.5% Triton-x, 5% normal horse serum (NHS) in 0.1M PBS was used for blocking. Each well, containing a single section, received 300 μl of solution. Sections were incubated in this blocking solution on a slow mixer for one hour. After blocking, the sections were again washed 3 times for 10 minutes each time in 0.1M PBS to ensure the removal of the detergent. Primary antibodies were added as listed above, prepared in 0.5% triton-X and 1% NHS in 0.1M PBS. The well plate was placed on a slow shaker in the refrigerator (4^{o}C) overnight. The following day, sections were washed 3 times for 10 minutes each wash in 0.1M PBS. Secondary antibodies were as follows, anti-mouse 568 (1:500; Invitrogen A11004), anti-chicken 488 (1:500; Invitrogen A11039), and streptavidin-conjugated 405 (1:500; Invitrogen S32351). The secondary antibodies were prepared in 0.5% triton-x and 1% NHS in 0.1M PBS. Sections were incubated in the secondary solution on a slow shaker for two hours. The sections received a final wash 3 times for 10 minutes each in 0.1M PBS and then were mounted to microscope slides using Vectashield medium. Coverslips were secured with nitrocellulose (clear nail polish).

One naïve TdxPV mouse was stained, the general procedure was the same, the only difference was replacing the primary GFP antibody with RFP antibody (1:500; Millipore B3528)

and secondary antibodies were changed to anti-mouse 488 (1:500; Invitrogen A11029) and anti-chicken 568 (1:500; Invitrogen A11041).

FLUORESCENT IMAGE ACQUISITION

All images were acquired using a Zeiss LSM 880 (Carl Zeiss Microscopy, White Plains, NY, USA) confocal microscope at 25x objective. Sections for analysis were chosen based on visual confirmation of the neocortex and then which area of the cortex included the greatest number of axotomy bulbs from the GAD67 channel. Two images were taken per animal.

QUANTIFICATION OF PERINEURONAL NETS

Pipsqueak software (Rewire AI, Portland, Oregon, United States) was used to quantify the intensity of WFA from GAD67 stained images. It is able to single out PNNs in an image and provide data such as pixel size of thr highlighted net and intensity of the WFA staining. WFA intensity data is given by “mean intensity” which is the intensity of each pixel summed then divided by the total number of pixels. By overlapping split images of WFA staining and GAD67 staining in Adobe Photoshop (San Jose, California, United State), cells that included PNNs and also an axotomy bulb could be easily identified and their intensity data could be extracted for analysis.

RESULTS

RxPV Animals

For each section, WFA showing PNNs was detected at 405nm, GAD67 showing axotomy at 568nm, and EYFP showing PV cells at 488nm. As previously discussed in the introduction, WFA is the most commonly used marker for PNNs. GAD67 has been recently confirmed as a marker of axotomy in GABAergic neurons (Vascak et al., 2018). As it turns out, channel rhodopsin in RxPV mice is unable to show intracellular contents of PV+ cells, making them extremely difficult to identify. Td tomato mice easily show PV+ soma when crossbred with Pv-cre mice but they were unfortunately unavailable to us at the time of the study. The EYFP channel was excluded from Figure 1 as it does not show anything of significance. The rest of the figure shows the WFA and GAD67 channels in an injured and sham animal. It should be noted that the sham animal does not show any axotomy bulbs as there are not any present due to the lack of injury.

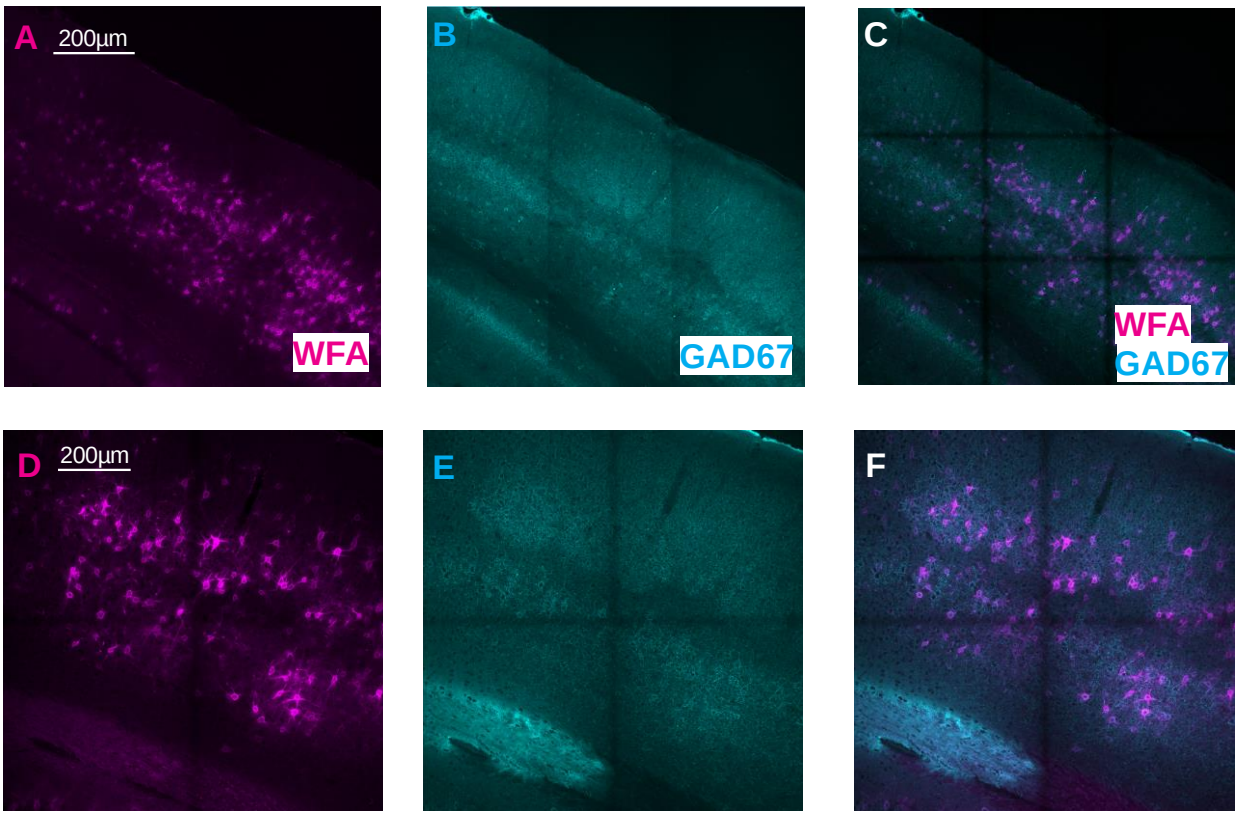

Figure 1. A. 3 Hour TBI mouse WFA channel showing perineuronal nets in a section of the neocortex. B. 3 hour TBI mouse GAD67 channel showing axontomy bulbs. This particular animal included 10 axotomy bulbs. C. Overlap of WFA and GAD67 channels in a 3 hour TBI mouse. D. A sham mouse WFA channel showing perineuronal nets in a setion of the neocortex. E. A sham mouse GAD67 channel. As you can see in this image, there are no axotomy bulbs because there was no injury preformed. E. Overlap of WFA and GAD67 channels in a sham mouse.

The axotomy bulbs are difficult to visualize in a zoomed out image but can be clearly seen in the zoomed in images in Figure 2, they are represented by the much brighter spots of cyan. Figure 2 also shows the range of general WFA intensity that is present with axotomy. Axotomy bulbs were found present in cells with strong WFA staining intensity, weak WFA intensity, and no WFA present at all.

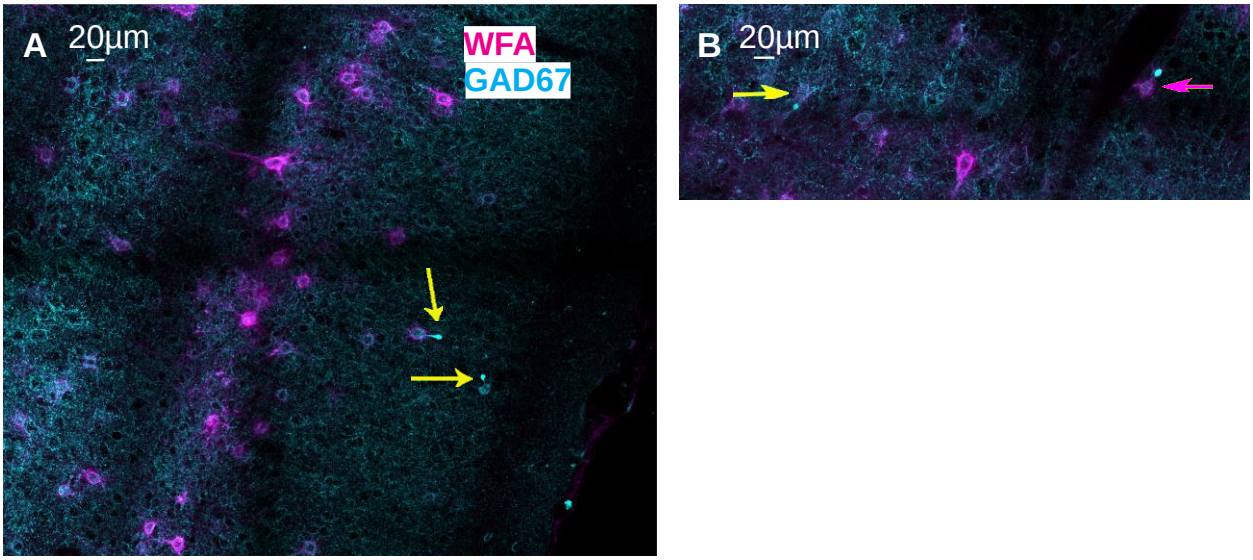

Figure 2. A. Zoomed in image of a 3 hour TBI mouse. Arrows are pointing to 2 axotomy bulbs. The top cell is surrounded by a PNN while the bottom cell is not surrounded by a PNN. B. Another zoomed in image of 2 axotomy bulbs. The bulb on the left with the yellow arrow is connected to a cell surrounded by a very weak PNN. The pink arrow on the right is a bulb connected to a cell with a stronger PNN.

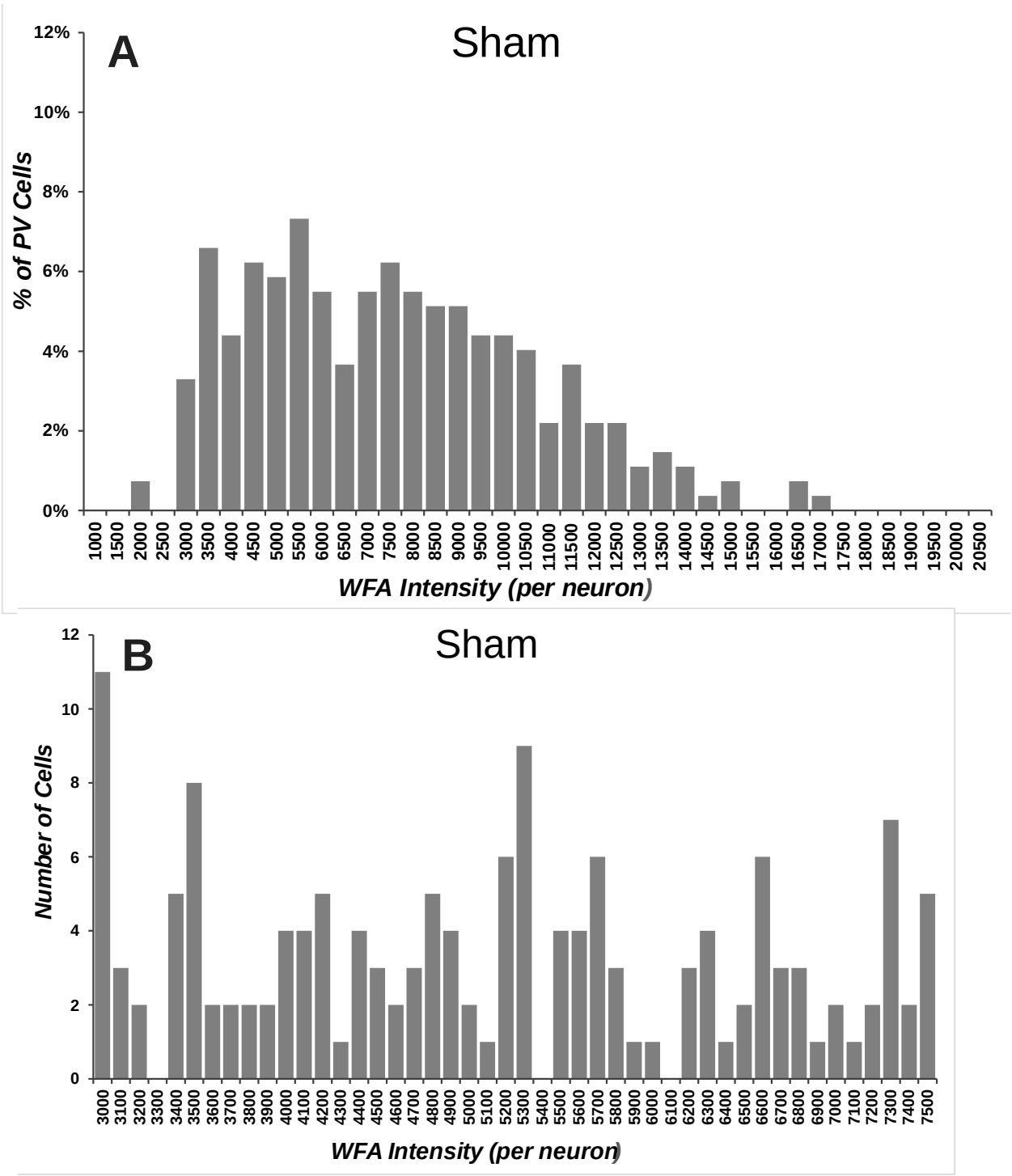

Figure 3. A. This histogram represents the distribution of intensity of PNN+ cells in the sham animals. There is a pretty average distribution into what is considered strong PNN intensity range. As sham animals these distributions can be considered "baseline" when comparing to distribution of intensity of injured animals. B. A finer distribution of intensity for Sham animals showing the natural break in intensity at 5500. This is the value that was chosen to be the little WFA cutoff because of this break.

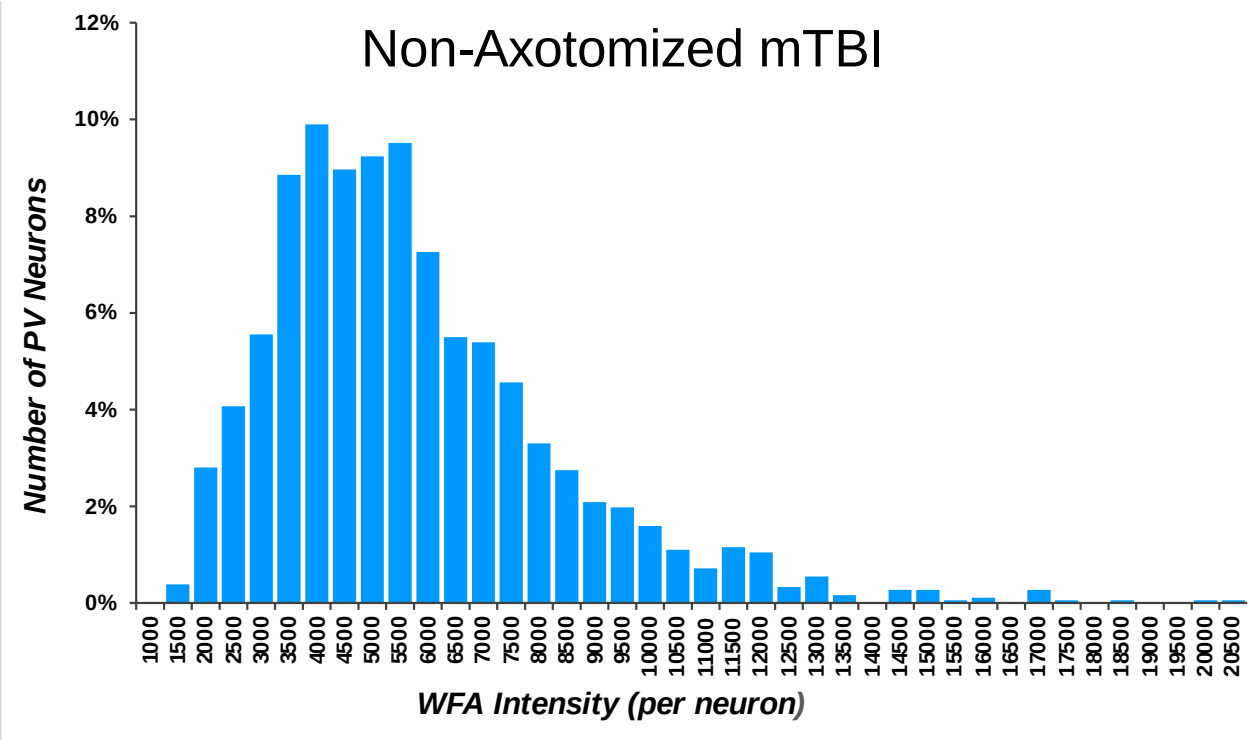

Figure 4. This histogram shows the distribution of mean intensity values of WFA staining in PNN+ cells after mTBI. There is a clear larger distribution of lower intensity values when compared to the Sham data

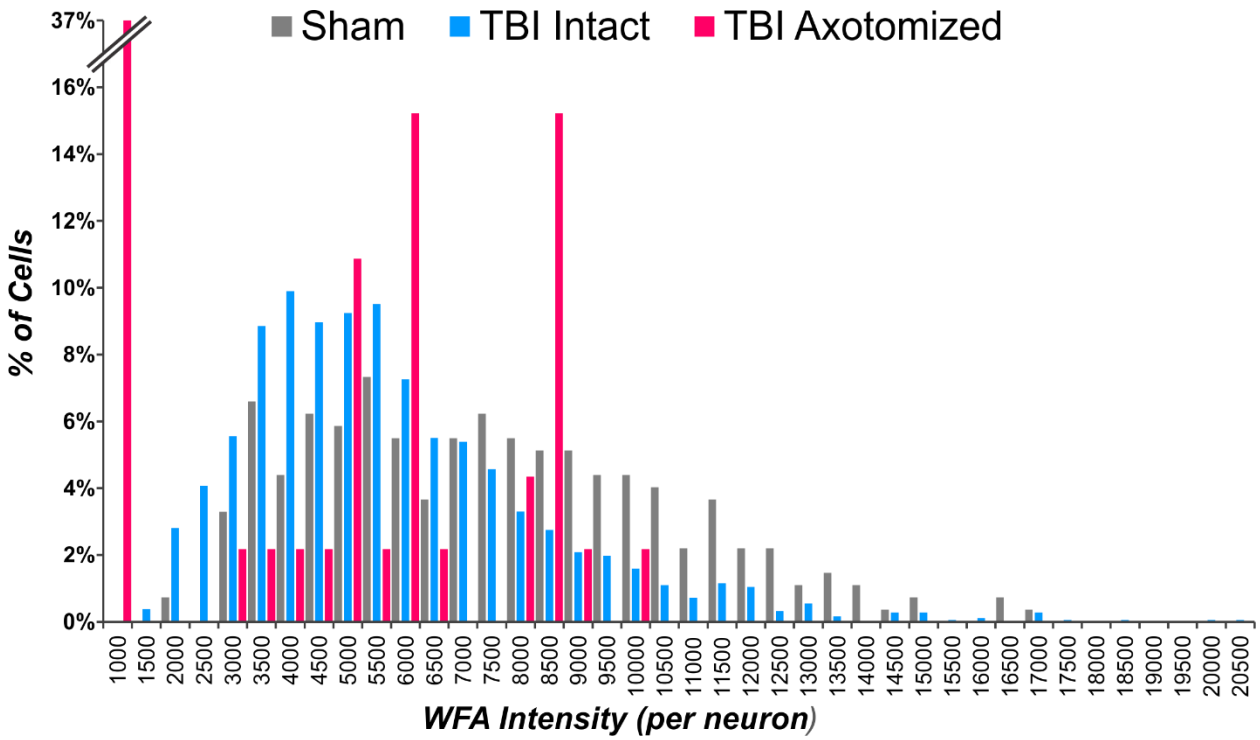

Figure 5. This Histogram shows the distribution of sham, non-axotomized after mTBI cells, and axotomized after mTBI cells.

Distribution of WFA Intensity of Sham and non-Axotomized After mTBI Cells

When examining the distribution of intensity among PNN+ cells between sham animals (Figure 3) and non-axotomized PNN+ cells after mTBI (Figure 4) there is a stark difference in the histograms. Not only do the non-axotomized cells have a much lower minimum intensity (1093.1) when compared to sham (1853.6), there is a much larger number of cells at a low intensity. Only 35% of the total sham cells are under the 5500 mean intensity threshold to be considered “little WFA” intensity while 60% of the non-axotomized mTBI cells are under this threshold. It was also found that sham animal cells have a more even distribution of intensity across intensity levels while the non-axotomized cells are much more concentrated in lower

intensity ranges. A value of 5500 was chosen to be “little WFA” as there is a natural break in sham distribution at this intensity value as seen in Figure 3. The distribution of cells were overlapped in Figure 5 so the dropoff of intensity in the non axotomized can be observed next to the sham distribution.

Average Intensity of Sham, Non-axotomized after mTBI, and axotomized after mTBI cells

Average intensity of the three classifications of axotomy, sham, non-axotomized after mTBI, and axotomized after mTBI, were plotted against each other (Figure 6, single ANOVA). Error bars, indicating the standard error of the mean (SEM), were included to the side of the graphed points as they were too small to be visible on the points themselves. Only average intensity points were plotted for the sham and non-axotomized after injury due to the very large number of data points. The “no WFA” axotomized cells were included in the graph with an intensity value of 0, there are 17 of these cells. It can be clearly seen that sham mice have a much higher average intensity (7374.9, $p < 0.01$) than both non-axotomized (5573.7, $p < 0.01$) and axotomized (3951.9, $p < 0.01$) after mTBI cells. Axotomized cells are found present in a wide range of intensities, but seem to cluster in certain intensity ranges and completely avoid others.

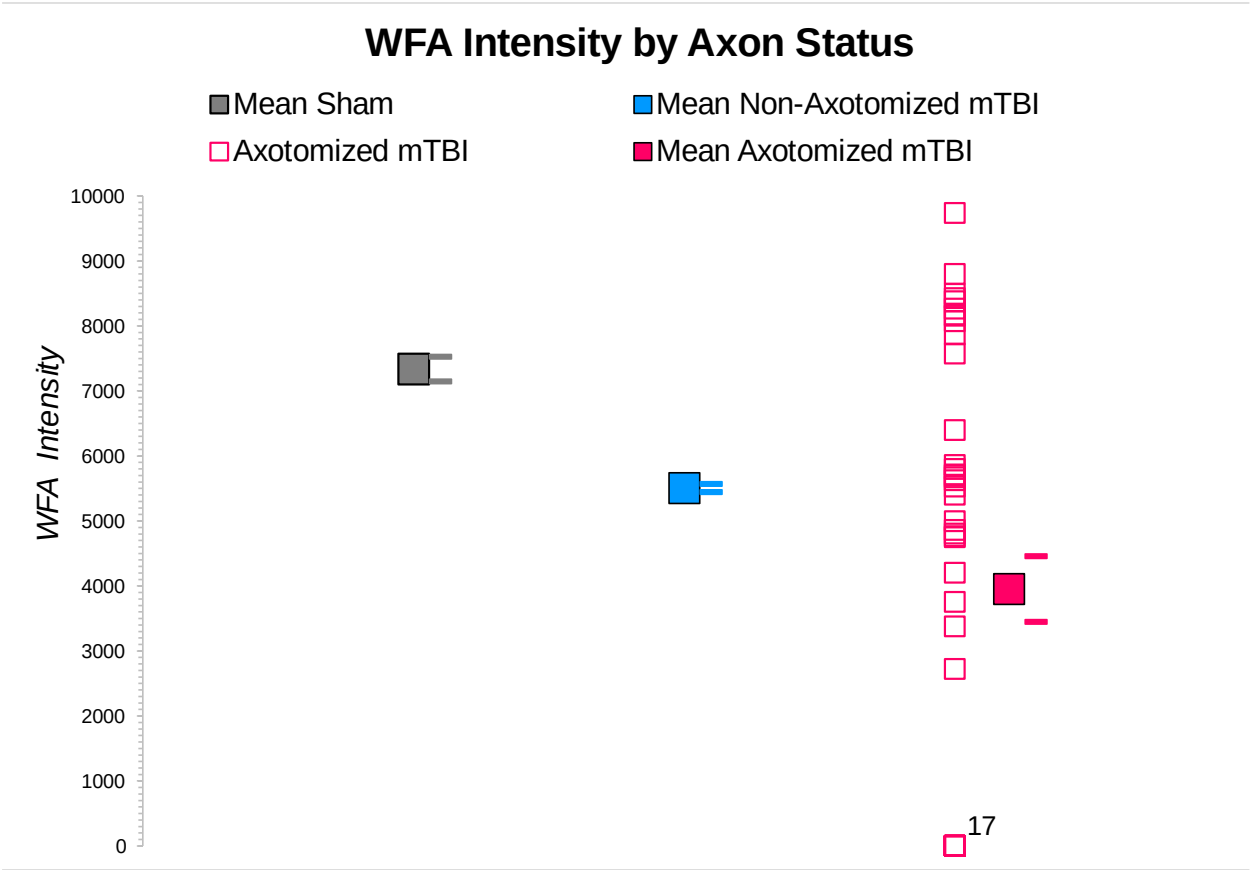

Figure 6. This graph shows intensity levels based on axotomy. The point immediately to the right of the Axotomized cell column is the average intensity for all of the axotomized cells. It is clearly represented that cells that went through TBI have, on average, a lower intensity level of WFA staining than sham animals. This suggets loss of WFA after injury. Also shown is that the axotomized PNN+ cells have a slightly higher average intensity than the non-axotomized cells suggesting that cells with a stronger, more mature PNN could be considered more susceptible to axonal injury.

Axotomized Cell Intensity

Cell counts of axotomized cells after mTBI were grouped into three classifications, no WFA, little WFA (mean intensity<5500) and WFA (mean intensity value>5500) (Figure 7). It should be noted that in this case mean intensity does not mean the same thing as average intensity from Figure 5, these mean intensity values are the intensity for each individual cell from the Pipsqueak program, calculated by adding the total intensity of each individual pixel and then dividing that sum by the toal number of pixels.The number of PV+ interneurons with no WFA and strong WFA are similar, while there were fewer PV+ cells present in the little WFA category. The number of sections represents the number of individual sections axotomy was found. A total of eight different animals were injured and two images were taken per animal for a total of sixteen sections. Plotting this with the number of individual cells shows that while no WFA and strong WFA axotomized cells were found in a majority of the captured images, low WFA non axotomized cells were not only found in the least amount of cells but were also not found in very many sections. It also shows lack of bias, as not all GAD67 axotomy staining came from one section. Four male and four female RxPV mice were used for the 3 hour injury group. No significant difference was found in WFA staining distribution between male and female so they were able to be in one data set

Percntage of Axotomized, Non-axotomized, and Sham Cells Based on General WFA Intensity

When examining axotomized PV+ cell WFA intensity, 46% had strong WFA intensity, 17% little WFA, and 37% no WFA. When grouping together little and no WFA because no WFA was given an intensity value of 0, little and no WFA, have the majority (54%) of axotomized cells. To go along with the histograms in Figures 3 and 4, Figure 8 also shows the

percentages of little and strong WFA intensity in sham and non-axotomized after mTBI PV+ neurons. The non-axotomized after injury PV+ neurons have a much higher percentage of little WFA (60%) than the sham neurons (35%).

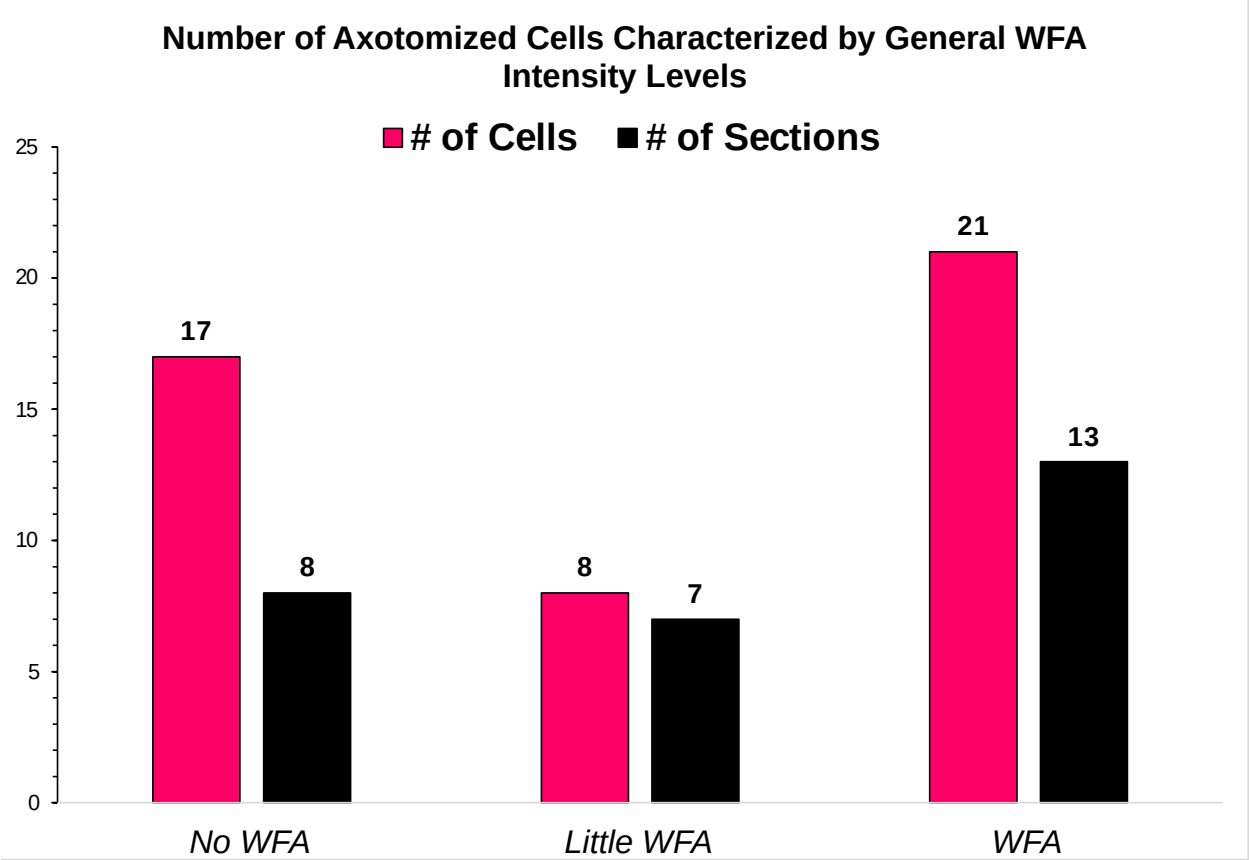

Figure 7. The bar graph above shows the number of axotomized cells distributed by general intensity levels. "little WFA" is considered anything under a mean intensty value of 5500 while WFA is anything above that value. Interestingly, most cells that are axotomized either have no WFA or strong WFA staining.

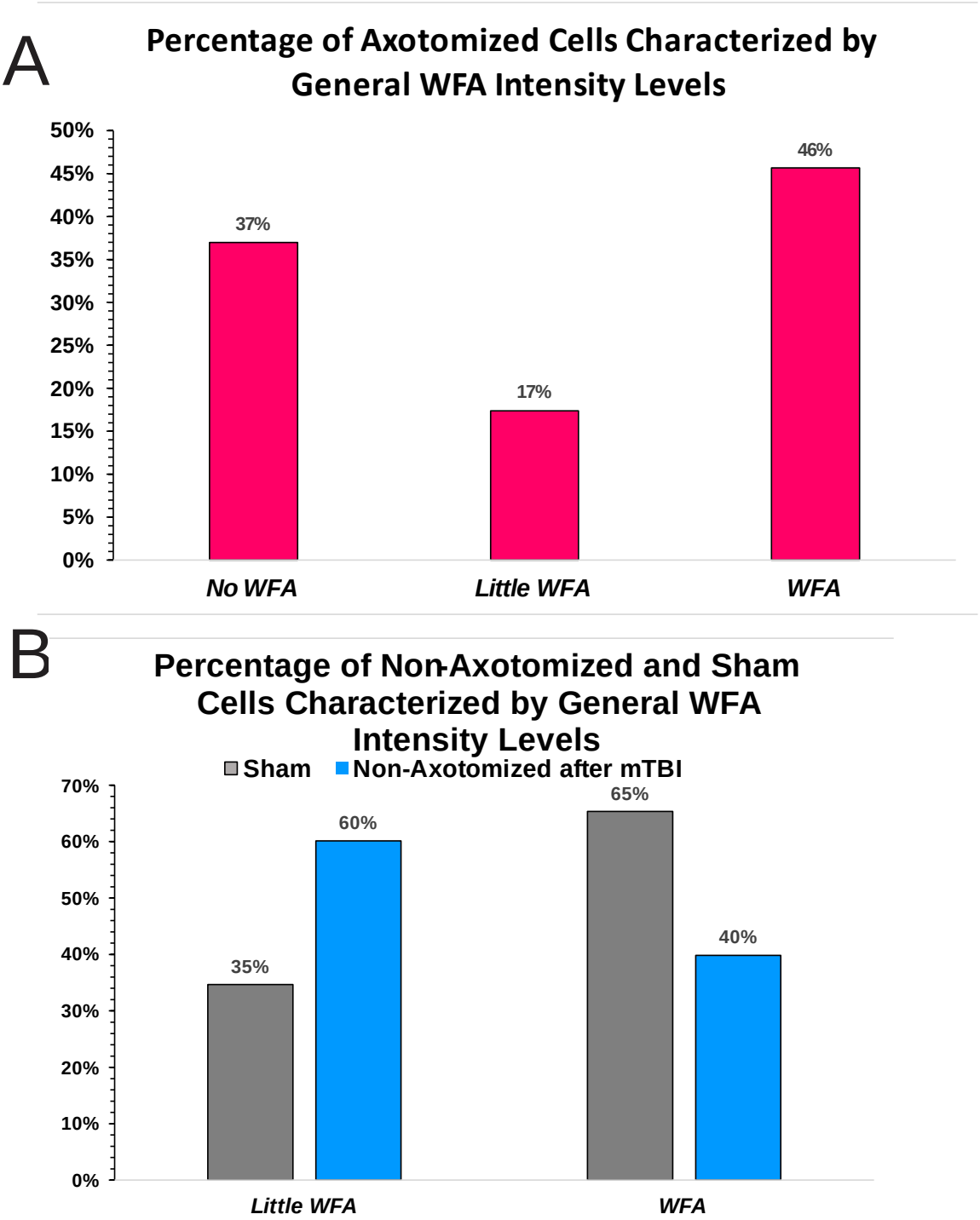

Figure 8. A. Percentage of axotomized PV+ cells characterized by intensity. Little WFA is intensity values less than 5500. B. Percentgaes of non-axotomized after mTBI and sham PV+ cells. Non-axotomized have a higher percentage of little WFA compared to sham indicating loss of PNNs.

TdxPV Naïve Animal

Due to lack of available animals, it was not possible to do this entire experiment with TdxPV mice. It was realized too late that the RxPV mice did not show the PV+ soma and no TdxPV mice were available at the time. One naïve TdxPV mouse was imaged (Figure 8), just to show what the images would have looked like with easily visible soma. Channels in this figure are the TdxPV Cre channel stained with RFP and detected at 588nm and again, WFA. The GAD67 channel was excluded in this Figure as being a naïve animal, there was no axotomy to show.

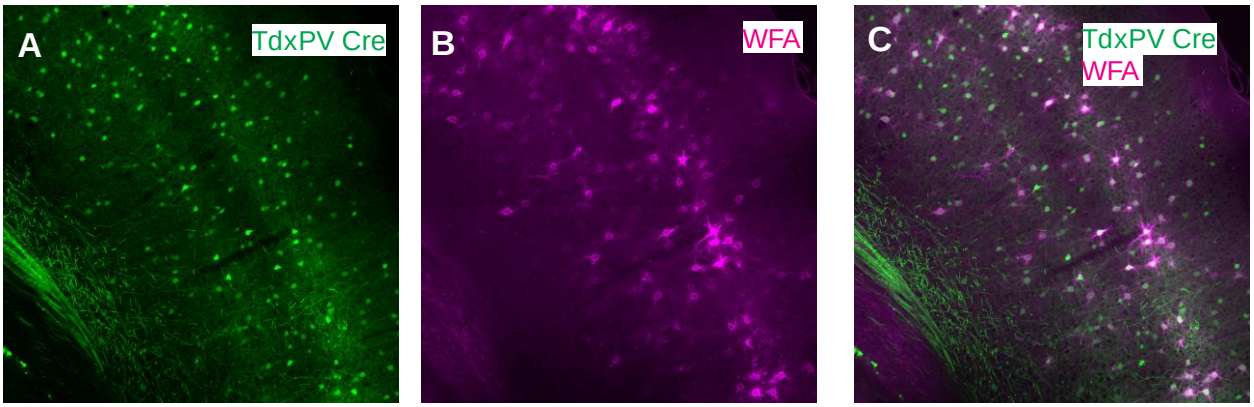

Figure 9. A. TdxPV Cre channel stained with RFP in a naive TdxPV Mouse. Can see that cell bodies are clearly labeled which was not seen in the RxPV mice. B. WFA channel showing PNNs in a naive TdxPV mouse. C. Overlap of TdxPV and WFA channels in a naive TdxPV mouse.

DISCUSSION

WFA Intensity of Sham vs. non-Axotomized Injured Cells

The main finding of this study is that after injury, intensity of WFA staining decreased in PV+ cells. Since the intensity of WFA staining has been shown to directly correlate to strength of PNNs, this shows that there was a loss of the PNNs after injury. Other studies have shown changes in inhibition indicating injury to PV+ cells using cFPI, (Lowenstein, Thomas, Smith, & McIntosh, 1992; Toth, Hollrigel, Gorcs, & Soltesz, 1997) however, all of these studies focused on the hippocampus and not the neocortex like this study; they also have varying ranges of severity of injury, the majority of them being classified as severe, not mild. There has been one other study done by Hseih in 2017 that studied loss of PNNs around PV+ cells in the neocortex using cFPI but their injury was classified as severe, using 2.0-2.5 atms of pressure during injury, indicating presence of a contusion (Hsieh et al., 2016). As previously discussed in the introduction, mTBI diagnoses in humans does not include any contusion injury, so while this study provided the same loss of WFA intensity as a result, it should not be considered the best model for mTBI in humans. In summary, while other studies have used the cFPI model of injury to show either injury to PV+ inhibitory neurons or loss of PNNs, this is the first study using the cFPI injury model with lack of contusion injury in the neocortex to show loss of PNNs after injury. TBI results in loss of synaptic density for up to 7 days after injury (Jamjoom, Rhodes, Andrews, & Grant, 2021). Regeneration of synaptic density could occur due to increased neuroplasticity from loss of PNNs. However, long-term loss of PNNs from mTBI could contribute to chronic symptoms seen in some mTBI patients as this could disrupt neuronal networks for long periods of time. It could also lead to more severe neural disorders that come

from a large disruption in excitatory to inhibitory ratios such as epilepsy if the neural networks are not repaired. It should be noted that this study only recorded intensity of WFA after 3 hours of injury, while loss of PNNs after only 3 hours of injury is a significant finding, other times should be recorded to see if results are different. One study done by Karetko-Sysa examined PNN loss after photothrombosis and found that in areas surrounding the ischemic lesion there was substantial PNN loss, but no evidence of any cell death markers associated with the downregulated PNNs (Karetko-Sysa, Skangiel-Kramska, & Nowicka, 2011). At 30 days post injury, the PNNs had only regenerated to 70% of original intensity when compared to sham, suggesting limited restoration even at long periods of time after injury. Prolonged downregulation of PNNs could be an attempt to maintain a high level of renewed synaptic plasticity after injury in order to promote generation of new GABAergic neurons after loss of inhibitory neurons. It is interesting that this study did not find an association between loss of PNNs and cell death. It could be possible the downregulation of PNNs is not a result of the injury itself but a protection mechanism to reintroduce plasticity after injury to reestablish properly functioning neural networks. However, it could be that prolonged downregulation of PNNs is only after severe injury resulting in a large amount of cell death like in the Karetko-Sysa study. Photothrombosis is obviously a completely different injury model that is much more severe and results in a large lesion and cell death, looking at PNN loss and possible regeneration at different time points after our model of mTBI should be considered as a possible future experiment.

No WFA, "Little WFA" and "Strong WFA" Cells

While this study was not able to visually confirm somata of PV+ cells due to the RXPV mice, previous studies have shown that in the neocortex, ranges of 70%-80%+ of PV+ cells are

also PNN+ (Lepine et al., 2022; Lupori et al., 2023). From this data, the assumption that the GAD67 axotomy bulbs with PNNs present are most likely PV+ neurons can be made. This study found that axotomized cells are most commonly surrounded by either no WFA or strong WFA, while axotomized cells surrounded by weak or "little" WFA were much more rare. Since the "no WFA" category is given an intensity value of 0, combining all axotomized cells that are under the 5500 range of low intensity gives 54% of axotomized cells have little or no WFA staining, showing that a majority of axotomized cells have a low intensity value. WFA intensity has a direct correlation to PNN strength meaning that the majority of cells that are axotomized have weaker or no PNNs. With the population of non-axotomized after mTBI also having a majority of PNNs having a low intensity level, the data is certainly not random even though PV+ cell could not be confirmed. As discussed in the previous discussion section, this study showed that our model of mTBI decreases the intensity of WFA intensity. If after injury, PNNs are decreased, and the majority of PV+ cells that show axotomy have low WFA intensity, this would suggest that after mTBI, cells are more susceptible to axonal injury. PNNs have been shown to provide some degree of protection to PV+ cells, so it makes sense from this study, that cells with lower WFA intensity, therefore weaker PNNs, are more susceptible to injury. Previous studies have shown that chondroitin sulphate proteoglycans (CSPGs), one of the main elements of PNNs, actually inhibit axonal repair after injury (Mowry et al., 2004). While PV+ neurons with no WFA or little WFA may have a higher likelihood of being injured, they may also have a higher chance of recovering compared to cells with strong PNNs. This could contribute to chronic injury from axonal injury to cells with stronger PNNs as they are not able to repair axons. Use of the enzyme chondroitinase ABC to break down CSPGs has been shown to enhance axonal sprouting after injury (Lee, 2009). This enzyme has only been used in humans in clinical trials and animal

studies, mostly with spinal cord injury. So, for the time being it is not really being used as a common treatment option for increasing axonal growth after injury. Another result of the Silver paper is an increase in plasticity after injury; since it has been shown that loss of PNNs leads to reintroducing neuroplasticity, it could be that this increase in plasticity comes from loss of PNNs. It is unknown if this increase in plasticity could aid in axonal injury recovering in PV+ neurons with strong PNNs.

No WFA Axotomized Cells

During this study, 17 cells were found axotomized that were not surrounded by any WFA, thus being represented with an intensity value of 0. It should be kept into consideration that in some cases the soma was not visible and thus may have actually been present in an adjacent section and may or may not have had WFA in that adjacent section. The RXPV mouse strain has the issue that PV terminals surrounding pyramidal neurons look similar to the PV staining in the membrane of PV somata. In addition, the GAD67 staining also does not stain the somata and typically in axotomized neurons the axon could not be followed back to the somata. All of these issues would be resolved with the use of TdXPV mice.

Future Studies

The most obvious study that should be conducted in the future is replicating this study with TdxPV mice so that the no WFA axotomy results can be confirmed. As discussed in the Introduction, a change in inhibition to excitation ratios when PV+ cells are injured has previously been demonstrated (Cardin, 2018; Sayin, 2003; Menuz, 2008). Using our injury model while studying excitatory post synaptic potentials (EPSPs) and inhibitory post synaptic potentials (IPSPs) of PV+ neurons can show whether the inhibitory to excitatory ratio changes

after our model of mTBI. This study only observed a 3-hour survival time after injury, other times should be examined to see if time after injury is a factor in the loss of WFA intensity. The mechanics of how PNNs adhere to PV+ cells should be studied, as in, what about mTBI actually makes PV+ cells lose PNNs.

BIBLIOGRAPHY

Ajmo, J. M., Eakin, A. K., Hamel, M. G., & Gottschall, P. E. (2008). Discordant localization of WFA reactivity and brevican/ADAMTS-derived fragment in rodent brain. *BMC Neurosci, 9*, 14. doi:10.1186/1471-2202-9-14

Baig, S., Wilcock, G. K., & Love, S. (2005). Loss of perineuronal net N-acetylgalactosamine in Alzheimer's disease. *Acta Neuropathol.(Berl), 110*(4), 393-401.

Bosiacki, M., Gassowska-Dobrowolska, M., Kojder, K., Fabianska, M., Jezewski, D., Gutowska, I., & Lubkowska, A. (2019). Perineuronal Nets and Their Role in Synaptic Homeostasis. *Int J Mol Sci, 20*(17). doi:10.3390/ijms20174108

Brown, T. E., & Sorg, B. A. (2023). Net gain and loss: influence of natural rewards and drugs of abuse on perineuronal nets. *Neuropsychopharmacology, 48*(1), 3-20. doi:10.1038/s41386-022-01337-x

Cabungcal, J. H., Steullet, P., Morishita, H., Kraftsik, R., Cuenod, M., Hensch, T. K., & Do, K. Q. (2013). Perineuronal nets protect fast-spiking interneurons against oxidative stress. *Proc Natl Acad Sci U S A, 110*(22), 9130-9135. doi:10.1073/pnas.1300454110

Caillard, O., Moreno, H., Schwaller, B., Llano, I., Celio, M. R., & Marty, A. (2000). Role of the calcium-binding protein parvalbumin in short-term synaptic plasticity. *Proc.Natl.Acad.Sci.U.S.A, 97*(24), 13372-13377.

Canas, N., Valero, T., Villarroya, M., Montell, E., Verges, J., Garcia, A. G., & Lopez, M. G. (2007). Chondroitin sulfate protects SH-SY5Y cells from oxidative stress by inducing heme oxygenase-1 via phosphatidylinositol 3-kinase/Akt. *J Pharmacol Exp Ther, 323*(3), 946-953. doi:10.1124/jpet.107.123505

Cardin, J. A. (2018). Inhibitory Interneurons Regulate Temporal Precision and Correlations in Cortical Circuits. *Trends Neurosci, 41*(10), 689-700. doi:10.1016/j.tins.2018.07.015

Carstens, K. E., Phillips, M. L., Pozzo-Miller, L., Weinberg, R. J., & Dudek, S. M. (2016). Perineuronal Nets Suppress Plasticity of Excitatory Synapses on CA2 Pyramidal Neurons. *J Neurosci, 36*(23), 6312-6320. doi:10.1523/JNEUROSCI.0245-16.2016

Crapser, J. D., Spangenberg, E. E., Barahona, R. A., Arreola, M. A., Hohsfield, L. A., & Green, K. N. (2020). Microglia facilitate loss of perineuronal nets in the Alzheimer's disease brain. *EBioMedicine, 58*, 102919. doi:10.1016/j.ebiom.2020.102919

Do, K. Q., Trabesinger, A. H., Kirsten-Kruger, M., Lauer, C. J., Dydak, U., Hell, D., . . . Cuenod, M. (2000). Schizophrenia: glutathione deficit in cerebrospinal fluid and prefrontal cortex in vivo. *Eur J Neurosci, 12*(10), 3721-3728. doi:10.1046/j.1460-9568.2000.00229.x

Dubisova, J., Burianova, J. S., Svobodova, L., Makovicky, P., Martinez-Varea, N., Cimpean, A., . . . Kubinova, S. (2022). Oral treatment of 4-methylumbelliferone reduced perineuronal nets and improved recognition memory in mice. *Brain Res Bull, 181*, 144-156. doi:10.1016/j.brainresbull.2022.01.011

Fawcett, J. W., Oohashi, T., & Pizzorusso, T. (2019). The roles of perineuronal nets and the perinodal extracellular matrix in neuronal function. *Nat Rev Neurosci, 20*(8), 451-465. doi:10.1038/s41583-019-0196-3

Frischknecht, R., Heine, M., Perrais, D., Seidenbecher, C. I., Choquet, D., & Gundelfinger, E. D. (2009). Brain extracellular matrix affects AMPA receptor lateral mobility and short-term synaptic plasticity. *Nat Neurosci, 12*(7), 897-904. doi:10.1038/nn.2338

Gardner, R. C., & Yaffe, K. (2015). Epidemiology of mild traumatic brain injury and neurodegenerative disease. *Mol Cell Neurosci, 66*(Pt B), 75-80. doi:10.1016/j.mcn.2015.03.001

Greer, J. E., Hanell, A., & Jacobs, K. M. (2013). **Increased Excitatory Synaptic Input to Axotomized and Intact Pyramidal Neurons After Mild Head Injury**. In *National Neurotrauma Symposium Abstracts* (Vol. 31, pp. D113). (Reprinted from: In File).

Greer, J. E., Hanell, A., McGinn, M. J., & Povlishock, J. T. (2013). Mild traumatic brain injury in the mouse induces axotomy primarily within the axon initial segment. *Acta Neuropathol, 126*(1), 59-74. doi:10.1007/s00401-013-1119-4

Greer, J. E., Povlishock, J. T., & Jacobs, K. M. (2011). Altered Physiology of Axotomized and Non-axotomized, Intact Pyramidal Neurons in a model of Diffuse Axonal Injury. In *National Neurotrauma Sympsoium Abstracts* (Vol. 29, pp. P320). (Reprinted from: In File).

Hanssen, K. O., & Malthe-Sorenssen, A. (2022). Perineuronal nets restrict transport near the neuron surface: A coarse-grained molecular dynamics study. *Front Comput Neurosci, 16*, 967735. doi:10.3389/fncom.2022.967735

Hartig, W., Meinicke, A., Michalski, D., Schob, S., & Jager, C. (2022). Update on Perineuronal Net Staining With Wisteria floribunda Agglutinin (WFA). *Front Integr Neurosci, 16*, 851988. doi:10.3389/fnint.2022.851988

Hobohm, C., Gunther, A., Grosche, J., Rossner, S., Schneider, D., & Bruckner, G. (2005). Decomposition and long-lasting downregulation of extracellular matrix in perineuronal nets induced by focal cerebral ischemia in rats. *J.Neurosci.Res., 80*(4), 539-548.

Hong, Y. C., Park, E. Y., Park, M. S., Ko, J. A., Oh, S. Y., Kim, H., . . . Ha, E. H. (2009). Community level exposure to chemicals and oxidative stress in adult population. *Toxicol Lett, 184*(2), 139-144. doi:10.1016/j.toxlet.2008.11.001

Hrabetova, S., Masri, D., Tao, L., Xiao, F., & Nicholson, C. (2009). Calcium diffusion enhanced after cleavage of negatively charged components of brain extracellular matrix by chondroitinase ABC. *J Physiol, 587*(Pt 16), 4029-4049. doi:10.1113/jphysiol.2009.170092

Hsieh, L. S., Wen, J. H., Claycomb, K., Huang, Y., Harrsch, F. A., Naegele, J. R., . . . Bordey, A. (2016). Convulsive seizures from experimental focal cortical dysplasia occur independently of cell misplacement. *Nat Commun, 7*, 11753. doi:10.1038/ncomms11753

Hutchins, J. B., & Barger, S. W. (1998). Why neurons die: cell death in the nervous system. *Anat Rec, 253*(3), 79-90. doi:10.1002/(SICI)1097-0185(199806)253:3<79::AID-AR4>3.0.CO;2-9

Jamjoom, A. A. B., Rhodes, J., Andrews, P. J. D., & Grant, S. G. N. (2021). The synapse in traumatic brain injury. *Brain, 144*(1), 18-31. doi:10.1093/brain/awaa321

Jang, H. J., Chung, H., Rowland, J. M., Richards, B. A., Kohl, M. M., & Kwag, J. (2020). Distinct roles of parvalbumin and somatostatin interneurons in gating the synchronization of spike times in the neocortex. *Sci Adv, 6*(17), eaay5333. doi:10.1126/sciadv.aay5333

Kabadi, S. V., Hilton, G. D., Stoica, B. A., Zapple, D. N., & Faden, A. I. (2010). Fluid-percussion-induced traumatic brain injury model in rats. *Nat.Protoc., 5*(9), 1552-1563.

Karetko-Sysa, M., Skangiel-Kramska, J., & Nowicka, D. (2011). Disturbance of perineuronal nets in the perilesional area after photothrombosis is not associated with neuronal death. *Exp Neurol, 231*(1), 113-126. doi:10.1016/j.expneurol.2011.05.022

Karube, F., Kubota, Y., & Kawaguchi, Y. (2004). Axon branching and synaptic bouton phenotypes in GABAergic nonpyramidal cell subtypes. *J Neurosci, 24*(12), 2853-2865.

Katz, D. I., Cohen, S. I., & Alexander, M. P. (2015). Mild traumatic brain injury. *Handb Clin Neurol, 127*, 131-156. doi:10.1016/B978-0-444-52892-6.00009-X

Kee, T., Sanda, P., Gupta, N., Stopfer, M., & Bazhenov, M. (2015). Feed-Forward versus Feedback Inhibition in a Basic Olfactory Circuit. *PLoS Comput Biol, 11*(10), e1004531. doi:10.1371/journal.pcbi.1004531

Kelly, J. C., Amerson, E. H., & Barth, J. T. (2012). Mild traumatic brain injury: lessons learned from clinical, sports, and combat concussions. *Rehabil Res Pract, 2012*, 371970. doi:10.1155/2012/371970

Lepine, M., Douceau, S., Devienne, G., Prunotto, P., Lenoir, S., Regnauld, C., . . . Vivien, D. (2022). Parvalbumin interneuron-derived tissue-type plasminogen activator shapes perineuronal net structure. *BMC Biol, 20*(1), 218. doi:10.1186/s12915-022-01419-8

Li, S., Mealing, G. A., Morley, P., & Stys, P. K. (1999). Novel injury mechanism in anoxia and trauma of spinal cord white matter: glutamate release via reverse Na+-dependent

glutamate transport. *J Neurosci, 19*(14), RC16. doi:10.1523/JNEUROSCI.19-14-j0002.1999

Lichvarova, L., Henzi, T., Safiulina, D., Kaasik, A., & Schwaller, B. (2018). Parvalbumin alters mitochondrial dynamics and affects cell morphology. *Cell Mol Life Sci, 75*(24), 4643-4666. doi:10.1007/s00018-018-2921-x

Lowenstein, D. H., Thomas, M. J., Smith, D. H., & McIntosh, T. K. (1992). Selective vulnerability of dentate hilar neurons following traumatic brain injury: a potential mechanistic link between head trauma and disorders of the hippocampus. *J Neurosci, 12*(12), 4846-4853.

Lupori, L., Totaro, V., Cornuti, S., Ciampi, L., Carrara, F., Grilli, E., . . . Pizzorusso, T. (2023). A comprehensive atlas of perineuronal net distribution and colocalization with parvalbumin in the adult mouse brain. *Cell Rep, 42*(7), 112788. doi:10.1016/j.celrep.2023.112788

Lusardi, T. A., Wolf, J. A., Putt, M. E., Smith, D. H., & Meaney, D. F. (2004). Effect of acute calcium influx after mechanical stretch injury in vitro on the viability of hippocampal neurons. *J Neurotrauma, 21*(1), 61-72. doi:10.1089/089771504772695959

Menuz, K., & Nicoll, R. A. (2008). Loss of inhibitory neuron AMPA receptors contributes to ataxia and epilepsy in stargazer mice. *J Neurosci, 28*(42), 10599-10603. doi:10.1523/JNEUROSCI.2732-08.2008

Miao, C., Cao, Q., Moser, M. B., & Moser, E. I. (2017). Parvalbumin and Somatostatin Interneurons Control Different Space-Coding Networks in the Medial Entorhinal Cortex. *Cell, 171*(3), 507-521 e517. doi:10.1016/j.cell.2017.08.050

Miyamae, T., Chen, K., Lewis, D. A., & Gonzalez-Burgos, G. (2017). Distinct Physiological Maturation of Parvalbumin-Positive Neuron Subtypes in Mouse Prefrontal Cortex. *J Neurosci, 37*(19), 4883-4902. doi:10.1523/JNEUROSCI.3325-16.2017

Morawski, M., Bruckner, M. K., Riederer, P., Bruckner, G., & Arendt, T. (2004). Perineuronal nets potentially protect against oxidative stress. *Exp Neurol, 188*(2), 309-315. doi:10.1016/j.expneurol.2004.04.017

Morawski, M., Reinert, T., Meyer-Klaucke, W., Wagner, F. E., Troger, W., Reinert, A., . . . Arendt, T. (2015). Ion exchanger in the brain: Quantitative analysis of perineuronally fixed anionic binding sites suggests diffusion barriers with ion sorting properties. *Sci Rep, 5*, 16471. doi:10.1038/srep16471

Mowry, B. J., Holmans, P. A., Pulver, A. E., Gejman, P. V., Riley, B., Williams, N. M., . . . Levinson, D. F. (2004). Multicenter linkage study of schizophrenia loci on chromosome 22q. *Mol.Psychiatry, 9*(8), 784-795.

Posmantur, R., Kampfl, A., Siman, R., Liu, J., Zhao, X., Clifton, G. L., & Hayes, R. L. (1997). A calpain inhibitor attenuates cortical cytoskeletal protein loss after experimental traumatic brain injury in the rat. *Neuroscience, 77*(3), 875-888. doi:10.1016/s0306-4522(96)00483-6

Prince, C., & Bruhns, M. E. (2017). Evaluation and Treatment of Mild Traumatic Brain Injury: The Role of Neuropsychology. *Brain Sci, 7*(8). doi:10.3390/brainsci7080105

Rankin-Gee, E. K., McRae, P. A., Baranov, E., Rogers, S., Wandrey, L., & Porter, B. E. (2015). Perineuronal net degradation in epilepsy. *Epilepsia, 56*(7), 1124-1133. doi:10.1111/epi.13026

Rowe, R. K., Harrison, J. L., Ellis, T. W., Adelson, P. D., & Lifshitz, J. (2018). Midline (central) fluid percussion model of traumatic brain injury in pediatric and adolescent rats. *J Neurosurg Pediatr, 22*(1), 22-30. doi:10.3171/2018.1.PEDS17449

Sayin, U., Osting, S., Hagen, J., Rutecki, P., & Sutula, T. (2003). Spontaneous seizures and loss of axo-axonic and axo-somatic inhibition induced by repeated brief seizures in kindled rats. *J.Neurosci., 23*(7), 2759-2768.

Shen, H. H. (2018). Core Concept: Perineuronal nets gain prominence for their role in learning, memory, and plasticity. *Proc Natl Acad Sci U S A, 115*(40), 9813-9815. doi:10.1073/pnas.1815273115

Sigal, Y. M., Bae, H., Bogart, L. J., Hensch, T. K., & Zhuang, X. (2019). Structural maturation of cortical perineuronal nets and their perforating synapses revealed by superresolution imaging. *Proc Natl Acad Sci U S A, 116*(14), 7071-7076. doi:10.1073/pnas.1817222116

Silverberg, N. D., Iverson, G. L., members, A. B. I. S. I. G. M. T. T. F., Cogan, A., Dams, O. C. K., Delmonico, R., . . . Zemek, R. (2023). The American Congress of Rehabilitation Medicine Diagnostic Criteria for Mild Traumatic Brain Injury. *Arch Phys Med Rehabil*. doi:10.1016/j.apmr.2023.03.036

Slaker, M. L., Harkness, J. H., & Sorg, B. A. (2016). A standardized and automated method of perineuronal net analysis using Wisteria floribunda agglutinin staining intensity. *IBRO Rep, 1*, 54-60. doi:10.1016/j.ibror.2016.10.001

Smith, D. H., Meaney, D. F., & Shull, W. H. (2003). Diffuse axonal injury in head trauma. *J.Head Trauma Rehabil., 18*(4), 307-316.

Sorg, B. A., Berretta, S., Blacktop, J. M., Fawcett, J. W., Kitagawa, H., Kwok, J. C., & Miquel, M. (2016). Casting a Wide Net: Role of Perineuronal Nets in Neural Plasticity. *J Neurosci, 36*(45), 11459-11468. doi:10.1523/JNEUROSCI.2351-16.2016

Toth, Z., Hollrigel, G. S., Gorcs, T., & Soltesz, I. (1997). Instantaneous perturbation of dentate interneuronal networks by a pressure wave-transient delivered to the neocortex. *J.Neurosci., 17*(21), 8106-8117.

Vascak, M., Jin, X., Jacobs, K. M., & Povlishock, J. T. (2018). Mild Traumatic Brain Injury Induces Structural and Functional Disconnection of Local Neocortical Inhibitory Networks via Parvalbumin Interneuron Diffuse Axonal Injury. *Cereb Cortex, 28*(5), 1625-1644. doi:10.1093/cercor/bhx058

Yang, S., Gigout, S., Molinaro, A., Naito-Matsui, Y., Hilton, S., Foscarin, S., . . . Fawcett, J. W. (2021). Chondroitin 6-sulphate is required for neuroplasticity and memory in ageing. *Mol Psychiatry, 26*(10), 5658-5668. doi:10.1038/s41380-021-01208-9